



ORIGINAL ARTICLE

Corrosion inhibition of iron in hydrochloric acid using pyrazole

S.S. Abdel-Rehim ^a, K.F. Khaled ^{b,c,*}, N.A. Al-Mobarak ^d

^a Ain Shams University, Faculty of Science, Chemistry Department, Abbassia, Cairo, Egypt

^b Electrochemistry Research Laboratory, Ain Shams University, Faculty of Education, Chemistry Department, Roxy, Cairo, Egypt

^c Materials and Corrosion Laboratory, Taif University, Faculty of Science, Chemistry Department, Taif, Hawiya 888, Saudi Arabia

^d Faculty of Science, Girls Section, Chemistry Department, Princess Nora bint Abdulrahman University, Riyadh, Saudi Arabia

Received 20 June 2010; accepted 25 June 2010

Available online 3 July 2010

KEYWORDS

Corrosion;
Inhibition;
Iron;
Hydrochloric acid;
Pyrazole

Abstract The corrosion and corrosion inhibition of iron in HCl solutions in the absence and presence of pyrazole (PA) were investigated by potentiodynamic polarization and electrochemical impedance spectroscopy (EIS). Changes in impedance parameters (R_{ct} and C_{dl}) were indicative of the adsorption of PA on the iron surface. The adsorption of PA is found to obey Langmuir adsorption isotherm. The study suggests that this compound is an anodic inhibitor.

© 2010 King Saud University. Production and hosting by Elsevier B.V. All rights reserved.

1. Introduction

All corrosion reduction processes are inhibitory (Hackerman, 1993). The use of chemical additions is one of the most practical methods for corrosion inhibition (Trabanelli, 1991). Acid solutions are generally used for the removal of

rust and scale in several industries (Bentiss et al., 1999). Hydrochloric acid is extensively used in industries, the most important fields of application being acid pickling, industrial acid cleaning, acid descaling and oil well acidizing. The continued manifestation of corrosion and corrosion products on iron and steel is still causing a lot of concern to corrosion scientists and engineers. Investigation into the mechanism of corrosion inhibition by certain nitrogen-containing compounds has continued to reveal interesting results (Khaled, 2009a,b, 2010a,b,c).

Pyrazole compounds have been hitherto little studied as corrosion inhibitors. Only derivatives of 3(5)-methylpyrazole have been examined as inhibitors for hydrogen sulfide corrosion of carbon steel (Proskurnya et al., 1982; Bocharnikov et al., 1979). This paper describes a study of the inhibition properties of 1H-Pyrazole (PA) for corrosion of pure iron (99.995) in 1 M HCl. The behaviour of this compound in 1 M HCl has been investigated and its inhibition efficiency has been determined by electrochemical methods (potentiodynamic polarization and electrochemical impedance spectroscopy).

* Corresponding author at: Electrochemistry Research Laboratory, Ain Shams University, Faculty of Education, Chemistry Department, Roxy, Cairo, Egypt.

E-mail address: khaledrice2003@yahoo.com (K.F. Khaled).



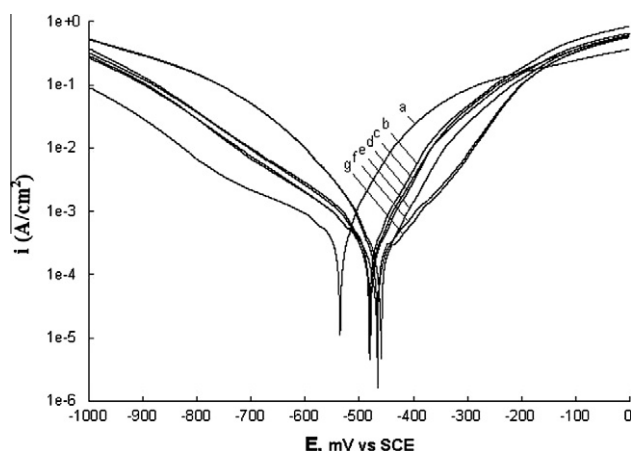


Figure 1 Potentiodynamic polarization curves of Iron immersed in 1 M HCl and different concentrations of PA. (a) Blank, (b) 1×10^{-3} , (c) 3×10^{-3} , (d) 5×10^{-3} , (e) 7×10^{-3} , (f) 9×10^{-3} , (g) 10×10^{-3} .

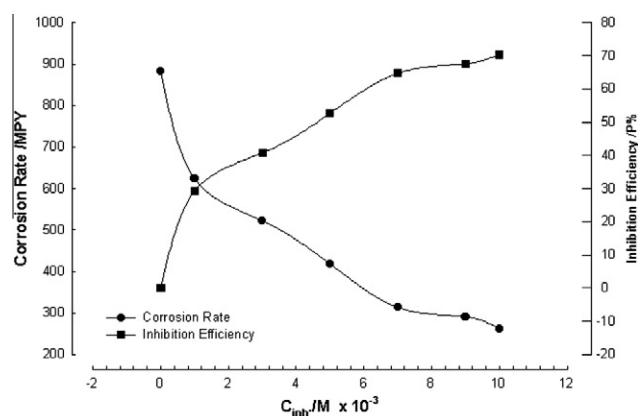


Figure 2 The corrosion rate/mpy and the inhibition efficiency $P\%$ for iron in 1 M HCl containing different concentrations of PA (from potentiodynamic data).

2. Experimental details

Iron specimens from Johnson Matthey (Puratronic, 99.995%) were mounted on Teflon. An epoxy resin was used to fill the space between Teflon and iron electrode in order to prevent crevice corrosion. The electrochemical measurements were performed in a typical three-compartment glass cell. The iron

specimen was the working electrode. Pt gauze was used as an auxiliary electrode and a saturated calomel electrode (SCE) as a reference electrode. The auxiliary electrode was separated from the working electrode compartment by fritted glass. The reference electrode was connected to Luggin capillary to minimize IR drop and chloride contamination.

Solutions were prepared from deionized water of resistivity 13 M Ω cm. The specimens were polished with emery papers up to 4/0 grit size, washed with double distilled water, etched in 12 M HCl for 10 min, and rinsed with double distilled water and then with acetone before immersion in the solutions. This procedure was used to ensure a reproducible starting surface state. The electrode potential was allowed to stabilize for 30 min before starting the measurements. All experiments were conducted at 25 °C. The solutions were prepared by mixing HCl (Fisher Scientific) with 1H-Pyrazole (PA) (Aldrich). The measurements were performed by means of an EG&G Princeton Applied Research Potentiostat/Galvanostat (PAR model 273) in combination with a Solarton 1250 frequency response analyzer and was used for polarization and capacitance measurements. The system was attached to a PC for collecting data. The potentiodynamic current – potential curves were recorded by changing the electrode potential automatically from -1000 to 0.000 mV with a scan rate of 1 mV s^{-1} . Electrochemical impedance spectroscopy (EIS) measurements were carried out in a frequency range of 10 KHz to 100 μ Hz using amplitude of 5 mV peak to peak using a.c. signal at open circuit potential. The softwares used in this study are electrochemical impedance software (Model 398), corrosion software (Model 352–252, version 2.23) and Equivalent circuit software (EQUIVCRT.PAS).

3. Results and discussion

Fig. 1 shows typical anodic and cathodic potentiodynamic polarization curves for iron in 1 M HCl in the absence and presence of various concentrations (10^{-3} – 10^{-2} M) of PA at 25 °C. Values of associated electrochemical parameters and the inhibition efficiency ($P\%$) are given in Table 1. The inhibition efficiency ($P\%$) is obtained from Eq. (1) Khaled, 2008

$$P\% = \left(\frac{i_{\text{corr}}^0 - i_{\text{corr}}}{i_{\text{corr}}^0} \right) \times 100 \quad (1)$$

where i_{corr}^0 and i_{corr} are the uninhibited and inhibited corrosion current densities, respectively, determined by extrapolation of Tafel lines.

Fig. 2 shows that increasing the inhibitor concentration decreases the corrosion rate and increases the inhibition efficiency. The decrease in i_{corr} with the inhibitor concentration

Table 1 Electrochemical parameters for iron in 1 M HCl with different concentrations of PA at 25 °C.

Conc./M	$i_{\text{corr}}/\mu\text{A.cm}^{-2}$	$-E_{\text{corr}}/\text{V}$	$-b_c/\text{V.dec}^{-1}$	$b_a/\text{V.dec}^{-1}$	C.R mpy	P %
Blank	965.2	0.535	0.131	0.091	882.5	-----
1×10^{-3}	681.7	0.482	0.139	0.095	623.3	29.37
3×10^{-3}	570.9	0.479	0.142	0.096	522.0	40.82
5×10^{-3}	455.7	0.479	0.144	0.096	416.7	52.78
7×10^{-3}	341.8	0.469	0.129	0.094	312.5	64.78
9×10^{-3}	317.9	0.466	0.129	0.094	290.7	67.58
10×10^{-3}	286.2	0.459	0.133	0.098	261.7	70.34

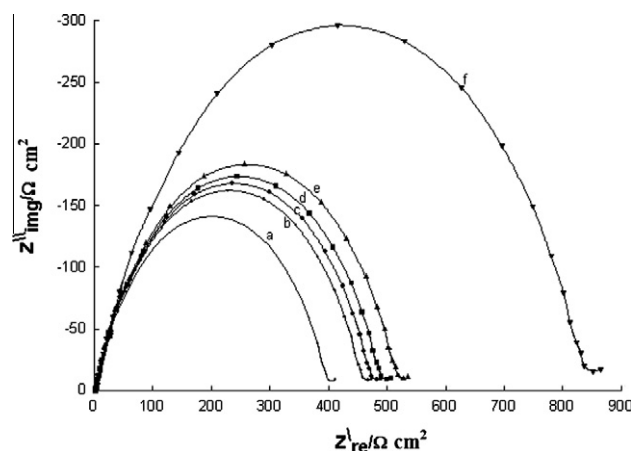


Figure 3 Impedance spectra recorded at different time of exposure of the working electrode in 1 M HCl: (a) 30, (b) 60, (c) 90, (d) 120, (e) 150, (f) 180 min.

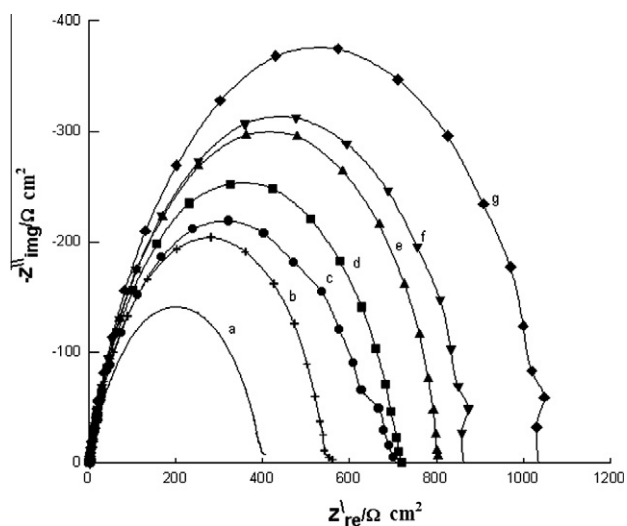


Figure 4 Complex-plane impedance of iron in 1 M HCl in the presence of different concentrations of PA at 25 °C. (a) Blank, (b) 1×10^{-3} M, (c) 3×10^{-3} M, (d) 5×10^{-3} M, (e) 7×10^{-3} M, (f) 9×10^{-3} M, (g) 10×10^{-3} M.

is associated with a shift of corrosion potential E_{corr} to less negative values. These results suggest that PA behaves mainly as anodic inhibitor. The approximately constant values of the Tafel slopes (near 0.09 V dec^{-1} for b_a and 0.13 V dec^{-1} for b_c) suggest that inhibition mechanism for PA involves a single reaction site blocking (Moretti and Quartarone, 1996; Hoar and Khera, 1960).

Fig. 3 shows the effect of the exposure duration in 1 M HCl on the impedance spectra (EIS). The results obtained provided the determination of the working electrode (WE) exposure time. This was required by comparative examination envisaged. The EIS were recorded after an exposure for 30, 60, 90, 120, 150, and 180 min. It is seen from the results presented in Fig. 3 that the diameter of the impedance semicircle depends on the duration of the WE exposure in the solution prior to the EIS recording.

Fig. 4 shows the complex – plane impedance plots of iron in 1M HCl without and with various concentrations of PA (10^{-3} – 10^{-2} M). The impedance diagrams obtained are not perfect semicircles and this difference has been attributed to frequency dispersion (Mansfeld et al., 1982). The charges transfer resistance R_{ct} values are calculated from the difference in impedance at lower and higher frequencies, as suggested by Tsuru et al. (1978). To obtain the double layer capacitance C_{dl} , the frequency at which the imaginary component of the impedance is maximum, $(-Z''_{\text{img}})$, is found and C_{dl} values are obtained from the Eq. (2) (Bentiss et al., 1999).

$$F(-Z''_{\text{max}}) = \frac{1}{2\pi C_{\text{dl}} R_{\text{ct}}} \quad (2)$$

Charge transfer resistance calculates the inhibition efficiency of the corrosion of iron, as in Eq. (3) (Khaled, 2008).

$$P\% = \frac{1/R_{\text{ct}}^0 - 1/R_{\text{ct}}}{1/R_{\text{ct}}^0} \times 100 \quad (3)$$

where R_{ct}^0 and R_{ct} are the charge transfer resistance values without and with inhibitor, respectively. The impedance parameters derived from this investigation are given in Table 2. From Table 2 it is found that by increasing the concentration of PA, corrosion rate ($1/R_{\text{ct}}$) decreases and the inhibition efficiency $P\%$ increases (Fig. 5).

Fig. 6 it is clear that by increasing the concentration of the inhibitor PA the double layer capacitance decreases C_{dl} .

Table 2 Impedance data of iron in 1 M HCl solution containing different concentrations of PA at 25 °C.

Inhibitor Conc./M	R_{ct} (Ohm cm^2)	C_{dl} ($\mu\text{F cm}^2$)	$P\%$
Blank	427.4	61.01	–
1×10^{-3}	571.4	44.1	25.20
3×10^{-3}	701.4	35.9	39.06
5×10^{-3}	754.8	33.4	43.37
7×10^{-3}	848.5	29.7	49.63
9×10^{-3}	928.3	27.1	53.95
10×10^{-3}	1114	22.6	61.63

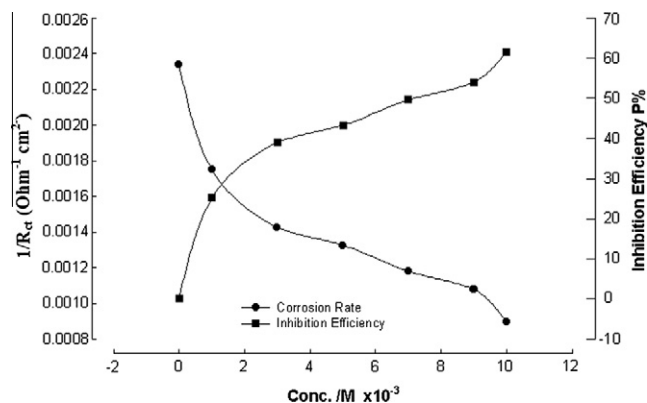


Figure 5 The inverse charge transfer resistance $1/R_{\text{ct}}$ and the inhibition efficiency $P\%$ for iron in 1 M HCl containing different concentrations of PA (from impedance data).

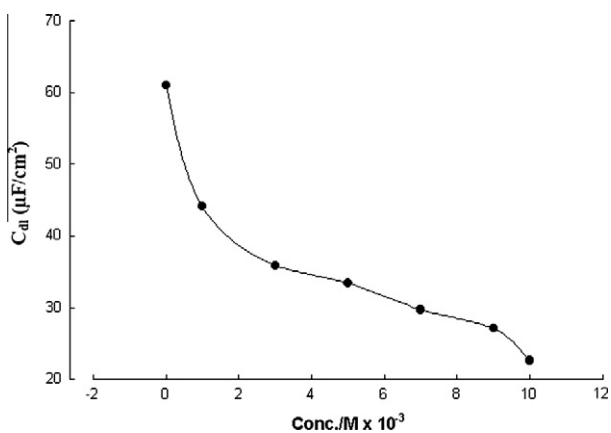


Figure 6 The double layer capacitance C_{dl} for iron in 1 M HCl containing different concentrations of PA.

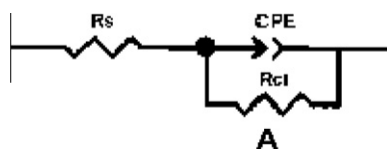


Figure 7 Equivalent circuit model for iron /1 M HCl interface.

Fig. 7 is the structure model of the interface iron/1 M HCl + PA. The EIS spectra in the presence of PA can be well described by this model. Some examples on applying non-least square fit (NLSF) are shown in Fig. 8. It is clear from these curves in Fig. 8 that there is some disagreement between the fit and the data at high and low frequency ranges. At higher frequencies the error in the fit is most likely due to the effect of stray capacities and uncompensated solution resistance of the system; however, the resistive component of the impedance can be estimated without much error as shown in the plot of the impedance in Fig. 8b.

The degree of surface coverage θ for different concentrations in HCl has been evaluated from electrochemical measurements, using Eq. (4) Khaled, 2008:

$$\theta = \frac{1/R_{ct}^0 - 1/R_{ct}}{1/R_{ct}^0} \quad (4)$$

The Plot of C_{inh}/θ versus C_{inh} yields a straight line Fig. 9, proving that the adsorption of PA from HCl solutions on the iron surface obeys the Langmuir adsorption isotherm.

The adsorption of PA on the metal surface can occur either directly on the basis of donor–acceptor interactions between the π -electrons of the heterocyclic compound and the vacant d-orbitals of iron surface atoms or the interaction of PA with already adsorbed chloride (Hackerman et al., 1966). The performance of pyrazole as an inhibitor in 1 M HCl can be explained in the following way. In aqueous acidic solutions, the pyrazole compound exists either as neutral molecules or

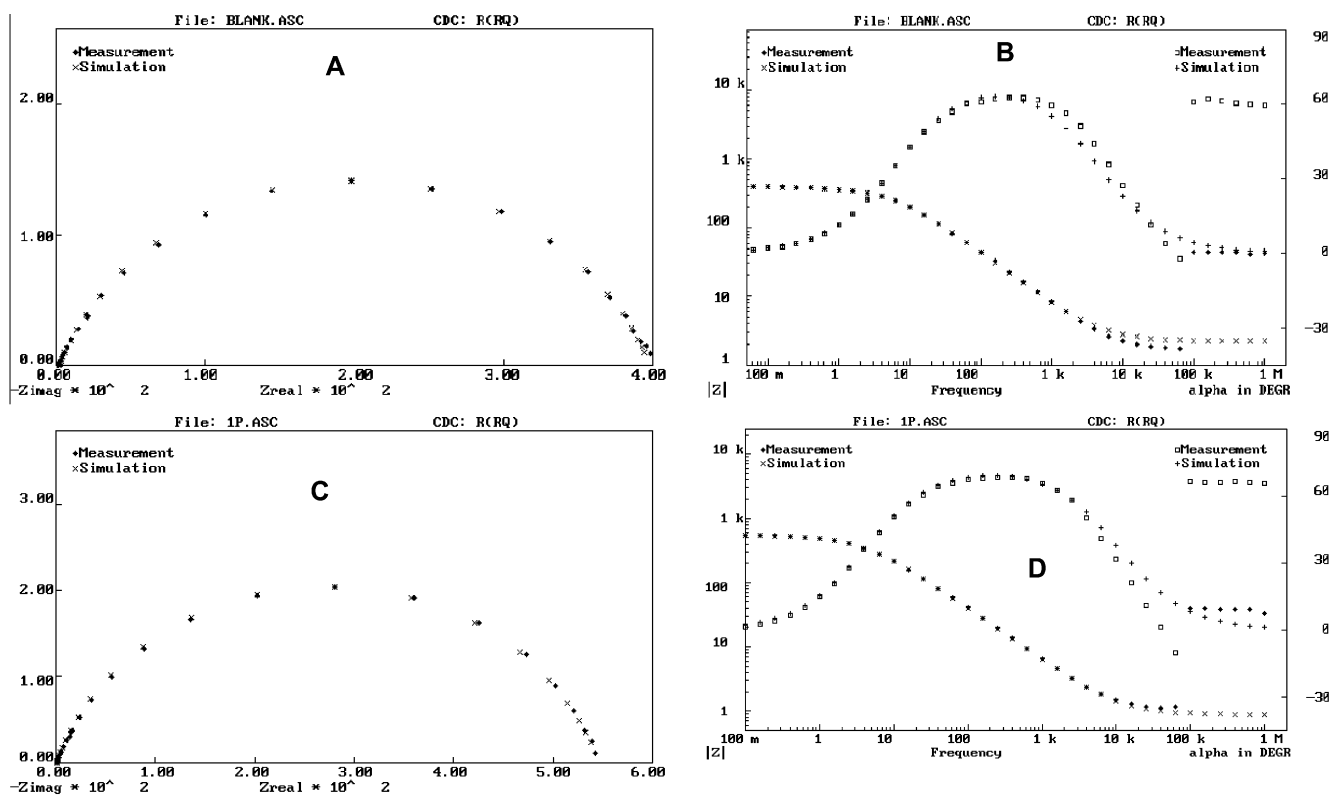


Figure 8 Impedance data for corroding iron at corrosion potential in 1 M HCl at 25 °C. Plot [A, C] shows the complex plan representation each data point corresponds to a different frequency; Plot [B, D] shows the magnitude and phase angel of the impedance as a function of frequency. Plot [A, B] for blank, and [C, D] for 10^{-3} M pyrazole/1 M HCl. (+) curves are the nonlinear regression to the data, open symbols are experimental data.

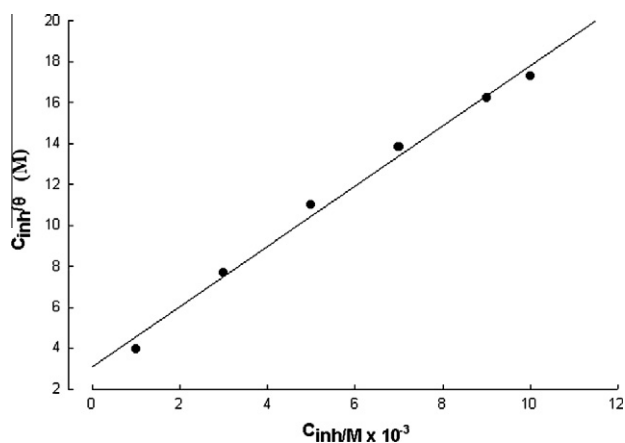


Figure 9 Langmuir adsorption plots for iron in 1 M HCl containing different concentrations of pyrazole.

in the form of cations. Amines may be adsorbed on the metal surface in the form of neutral molecules, involving the displacement of water molecules from the metal surface and sharing of electrons between the nitrogen atoms and the metal surface (Hackerman and Makrides, 1955). Amines and heterocyclic nitrogen compounds may also adsorb through electrostatic interactions between the positively charged nitrogen atom and the negatively charged metal surface (Mann, 1936). The presence of lone pairs and π -electrons of the pyrazole compound enhanced the inhibitory effect of this compound.

4. Conclusion

It can be concluded that:

1. PA inhibits the corrosion of iron in HCl solutions.

2. PA behaves as an anodic inhibitor.

3. The adsorption of PA from HCl obeys Langmuir adsorption isotherm.

References

- Bentiss, F., Lagrenee, M., Traisnel, M., Hornez, L.C., 1999. *Corros. Sci.* 41, 789–803.
- Bocharnikov, A.I., Sorochenko, A.A., Seraya, V.I., Dubrovskaya, V.A., 1979. *Zashch. Met.* 15, 705.
- Hackerman, N., 1993. *Reviews on Corrosion Inhibitor Science and Technology*. NACE, pp. I-1-1
- Hackerman, N., Makrides, A.C., 1955. *J. Phys. Chem.* 59, 707.
- Hackerman, N., Snavely Jr., E., Payne Jr., J.S., 1966. *Electrochem. Soc.* 113, 677.
- Hoar, T.P., Khera, R.P., 1960. In: *Proceedings of the 1st European Symposium on Corrosion Inhibitors*, vol. 73. University of Ferrara, Ferrara, Italy.
- Khaled, K.F., 2008. *Mater. Chem. Phys.* 112, 104–111.
- Khaled, K.F., 2009a. *J. Appl. Electrochem.* 39, 429–438.
- Khaled, K.F., 2009b. *Electrochim. Acta* 54, 4345–4352.
- Khaled, K.F., 2010a. *J. Electrochem. Soc.* 157, C116–C124.
- Khaled, K.F., 2010b. *Appl. Surf. Sci.* 256, 6753–6763.
- Khaled, K.F., 2010c. *Electrochim. Acta* 55, 5375–5383.
- Mann, C.A., 1936. *Trans. Electrochem. Soc.* 69, 105.
- Mansfeld, F., Kending, M.W., Tsai, S., 1982. *Corrosion* 38, 570.
- Moretti, G., Quartarone, G., 1996. *A Tassan and Zingales. Electrochim. Acta* 41, 1971.
- Proskurnya, L.V., Fedorv, Yu.V., Skvortsova, G.G., Es'Kova, L.A., 1982. *Zashch. Met.* 18, 930–932.
- Trabanelli, G., 1991. *Corrosion* 47, 410.
- Tsuru, T., Haruyama, S., Boshoku, J., 1978. *Jpn. Soc. Corros. Eng.* 27.